

Synthesis and Photocatalytic Activity of Ruthenium-Titania for Enhanced Decolorization of Malachite Green under Visible Light Illumination

Aldrin Lorrenz A. Chan, Sarah Jane C. Lopez, Arvie Victor M. Masangkay, and Lorico DS. Lapitan Jr

Abstract—The photodecolorization of malachite green (MG) dye was effectively done using Ruthenium-doped TiO₂ photocatalysts under visible light illumination. X-ray diffraction analysis revealed that anatase and rutile peaks were both found in undoped TiO₂ while only anatase peaks were present in Ru-doped TiO₂ systems which were calcined at 500°C. The 0.008 Ru-TiO₂ photocatalysts calcined at 300°C showed broader peaks compared to those calcined at 500°C. Further increase of calcination temperature to 700°C promotes the transformation of anatase to rutile peaks. The photocatalytic activity of TiO₂ was found to increase with the addition of Ruthenium ions, from 20% for undoped TiO₂ to 87% for 0.80 Ru-doped TiO₂. The maximum photocatalytic removal of MG dye was achieved using 1.50 g·L⁻¹ of catalyst loading for 0.008 Ru-doped TiO₂. The TiO₂ photocatalysts prepared at a calcination temperature of 500°C showed higher photodecolorization efficiency compared to those calcined at 300°C and 700°C. Kinetic studies revealed that the photodecolorization of MG using Ru-doped TiO₂ followed a first order kinetics.

Index Terms—Photocatalytic, decolorization, malachite green, Titania.

I. INTRODUCTION

The expansion of chemical process industries has increased the emission of various pollutants that eventually accumulate in the ecosystem. Among these pollutants are an estimated 280,000 tons of synthetic-dye effluents discharged annually [1], [2]. Synthetic dyes are problematic because they are non-biodegradable and blocks sunlight, thus endangering aquatic life through the inhibition of photosynthesis [3]. Malachite green (MG) is a triarylmethane dye (Fig. 1) widely used as a colorant in textile, paper, and leather manufacturing. It is also utilized as a biocide and antifungal agent in aquaculture, and as a coloring agent and additive in food. MG is environmentally persistent and has been identified as carcinogenic, mutagenic, teratogenic, and a culprit to developmental abnormalities among mammals [4]. Its toxicity increases with exposure time, concentration, and temperature. MG is a toxin that affects the spleen, kidney, liver, and heart in humans [5], [6].

Manuscript received December 7, 2021; revised January 11, 2022.

A. A. Chan is with the Department of Chemical Engineering, Faculty of Engineering, University of Santo Tomas, Manila, Philippines (e-mail: aachan@ust.edu.ph).

S. J. Lopez and A. V. Masangkay were with the Department of Chemical Engineering, Faculty of Engineering, University of Santo Tomas, Manila, Philippines.

L. D. Lapitan Jr. is with the Department of Chemical Engineering, Faculty of Engineering, University of Santo Tomas, Manila, Philippines and Research Center for the Natural and Applied Sciences, University of Santo Tomas (e-mail: ldlapitan@ust.edu.ph).

Due to its toxicity, low biodegradability, and high degree of color intensity, conventional wastewater treatment technologies are ineffective for synthetic dyes such as MG [7]. Hence, technologies involving advanced oxidation processes (AOPs) such as TiO₂ photocatalysis emerged [8]. Aside from its superior capacity to break down organic compounds photocatalytically, TiO₂ is preferred among other photocatalysts reported because it is relatively cheaper, chemically stable, highly oxidizing, and non-toxic [9]. However, due to its wide band-gap energy, TiO₂ only absorbs UV light and is not well suited under visible light conditions. To shift the absorption band to the visible region, metal or metal oxide doping of TiO₂ have been proposed [10]-[13].

Several studies have found that adding transition metal ions to TiO₂-based catalytic systems can significantly improve their efficiency [10]-[13]. Chiou & Juang (2007) reported a significant shift of the absorption band to the visible region for 0.072 mol% Pr-doped TiO₂ compared to undoped TiO₂. Furthermore, 99% phenol degradation (with initial concentration of 12.5 mg/L) was achieved using 1.0 g/L dosage of 0.072 mol% Pr-doped TiO₂ after 2 hours of UV irradiation. In a study conducted by Senthilnathan and colleagues (2010), the photocatalytic activity of TiO₂ increased upon addition of Ru metal. The removal efficiency of melsulfuronmethyl (MSM) also increased from 40% when undoped to 80% when doped with Ru. Moreover, an increase in calcination temperature of TiO₂ from 300°C to 900°C resulted in an increase in the degradation efficiency of MSM. However, no significant change in the MSM degradation efficiency was observed beyond the optimal dosage of 0.5 g/L. Joice and colleagues (2012) studied the effects of Ru-doping to TiO₂ in the decolorization of Amidoblack-10B (AB-10B) and found out that the addition of Ru increased visible light absorption and decreased the electron-hole pairs recombination rate, which enhanced photocatalytic activity. Using 1% Ru/TiO₂ prepared by simple sol-gel method, complete decolorization of AB-10B was achieved at 210 minutes under UV radiation. Elsalamony and Mahmoud (2017) investigated the photocatalytic activity of Ru-doped TiO₂ for the photocatalytic degradation of 2-chlorophenol (2-CP) and achieved a maximum of 2-CP photodegradation efficiency of 53% using 2% Ru/TiO₂ with catalyst loading of 4 mg·L⁻¹ under visible light. Moreover, they reported that Ru-doping of TiO₂ resulted in an increase in pore volume and surface area. In this study, TiO₂ nanoparticles were prepared by sol-gel method and doped with Ru ions. The synthesized Ru-doped TiO₂ were characterized using XRD, SEM-EDX and FT-IR. The effects of dopant concentration, photocatalyst loading, and calcination temperature to the photocatalytic

activity were investigated. The evaluation of photocatalytic activity and kinetic studies were performed through the photodecolorization of MG under visible light illumination. The evaluation of proposed photodecolorization mechanism and determination of kinetic parameters constitute the aim of this work which was previously not reported for MG.

II. METHODOLOGY

A. Chemicals and Reagents

Reagent grade malachite green (MG) was obtained from Alyson's Chemical Co., Philippines and was used without any further purification. Titanium isopropoxide (>99%) and ruthenium chloride hydrate are analytical grade and were purchased from Sigma-Aldrich, Singapore. Ethanol, acetic acid and perchloric acid are analytical reagent grade, and were purchased from Scharlau Chemical Co., Spain. Stock solutions containing 50 ppm of MG were prepared using distilled water and protected from light. Experimental solutions of desired concentrations were obtained further by dilution. The structure of malachite green is shown in Fig. 1.

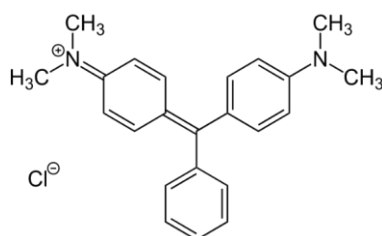


Fig. 1. Structure of Malachite Green (MG).

B. Synthesis of Undoped and Ruthenium Doped TiO₂ Photocatalysts

The typical sol-gel procedure for undoped TiO₂ and Ru-doped TiO₂ was performed as follows: Solution A was prepared by mixing 18.0 mL titanium (IV) isopropoxide with 25.0 mL ethanol. Solution B was also prepared by mixing 4.6 mL acetic acid, 2.0 mL water, and 25.0 mL ethanol. Solution B was then added drop wise to Solution A under constant stirring until a clear solution was achieved. The pH of the solution was adjusted to pH 2.2 by dropwise addition of perchloric acid. The prepared solution was placed in an oven at a temperature of 70°C for a period of 7 hours for the gelation process. The gel was dried at 100°C, crushed into fine powder using mortar and pestle, and calcined in a muffle furnace at 500°C for 5 hours. The typical synthesis preparation of Ru-doped TiO₂ involved adding a requisite amount of 0.10 M ruthenium chloride solution to Solution B to obtain a 0.002, 0.005, and 0.0080 mol Ru:TiO₂ mol ratio.

C. Material Characterization of Photocatalysts

1) *Powder X-ray diffraction*: The crystal phase composition of the prepared photocatalysts were determined using powder X-ray diffraction. Powder XRD measurements were carried out at room temperature using a Rigaku D/MAX-RB diffractometer operated with Cu K α source ($\lambda = 0.1541$ nm). The diffraction data was collected using a continuous scan mode with speed of 4° (2 θ)/min in the region 10-80° with a step size of 0.04°. The accelerating voltage and

applied current was 40 kV and 50 mA, respectively. The crystallite size of the catalysts was determined using the Scherrer equation (1).

$$D = \frac{K}{\beta \cos \theta} \quad (1)$$

where D refer to the crystallite size, K is a constant (0.89), λ is the wavelength of the Cu K α radiation, β is the line broadening full width at half-maximum (FWHM) peak height in radians, and θ is the Bragg angle. The most intense peak in the XRD spectrum which is the anatase phase 101 ($2\theta = 25.42^\circ$) (JCPDS # 21-1272) was used for calculating the average crystallite size of the photocatalysts. The percentages of rutile from X-ray diffraction intensities and the mass fraction of rutile, X_R was determined using (2).

$$X_R = \frac{I_R}{0.8I_A + I_R} \quad (2)$$

where I_R is the peak intensity of the principal rutile peak (110) ($2\theta = 27.4^\circ$) and I_A is the peak intensity of the principal anatase peak (101) ($2\theta=25.3^\circ$) [14].

2) *Scanning electron microscopy and energy dispersive spectroscopy*: The surface morphology and elemental composition of the as-prepared TiO₂ photocatalysts were investigated using Scanning Electron Microscopy (JEOL 5310) equipped with Energy Dispersive Spectroscopy (EDS) system (Ametek EDAX Element).

3) *Fourier transform - infrared spectroscopy (FT-IR)*: The FT-IR spectra were collected at room temperature using a Perkin Elmer Spectrum 2 FT-IR spectrometer. The spectrum of pure KBr cell was first collected as background. Then, the prepared catalysts were mixed with KBr (~0.5: 99.5), ground in an agate mortar and pressed to obtain a transparent KBr – photocatalyst film. The FT-IR spectra of the film was recorded in a working range of 350 – 4000 cm⁻¹ wavenumbers.

D. Photodecolorization Studies of Malachite Green Using UV-Vis Spectrophotometer

The photocatalytic decolorization of 50 ppm MG was performed in a batch operating mode and under ambient temperature $30 \pm 2^\circ\text{C}$ as shown in Fig. 2. A measured amount (0.50 g·L⁻¹ to 3.0 g·L⁻¹) of photocatalyst powder was dispersed in 1.0 L of 50 ppm MG solution. The photoreactor consist of a 150 W tungsten lamp placed inside a double wall jacketed glass vessel. Prior to irradiation, the solution containing the TiO₂ catalyst was stirred for 30 minutes under dark conditions to achieve adsorption–desorption equilibrium. The temperature of the system was kept constant by recirculating cooling water. The entire set-up was enclosed by an aluminum foil reflector to optimize visible light irradiation and to prevent interference from outside light. A 10.0 mL aliquot was withdrawn every after 15 minutes and centrifuged to separate the photocatalysts. The supernatant liquid was filtered through a 0.22 μm Sartorius® membrane filter and its absorbance at 616 nm was recorded using a UV-Vis spectrophotometer (Hitachi U-5100). The photodecolorization efficiency (η) or percent removal of MG

was calculated using (3).

$$\eta = \left[\frac{C_o - C}{C_o} \right] \times 100 \quad (3)$$

where C_o is the original concentration of malachite green solution and C is the absorbance of MG solution at time t .

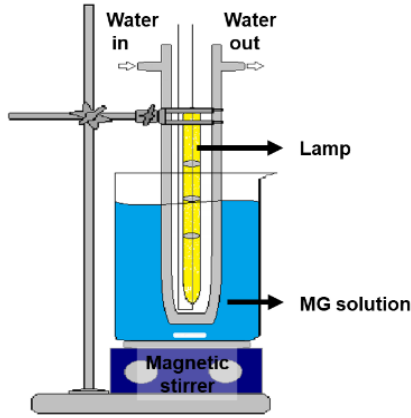


Fig. 2. Schematic diagram of glass double jacketed photoreactor used in this study.

III. RESULTS AND DISCUSSION

A. Characterization of Photocatalysts

1) X-ray diffraction

Fig. 3 shows the XRD patterns for the as-synthesized TiO_2 photocatalysts. All peaks were identified and indexed using the Joint Committee for Powder Diffraction studies (JCPDS) and the corresponding crystal planes are indicated in Fig. 3. The XRD pattern for undoped TiO_2 in Fig. 3a shows peaks at $2\theta = 27.4^\circ, 36.1^\circ, 39.2^\circ, 41.3^\circ,$ and 44.1° which correspond to rutile (JCPDS card no. 21-1276). The other peaks in the diffractogram are similar to the previously reported XRD pattern for undoped TiO_2 [15]-[17]. This implies a successful synthesis of the TiO_2 and confirms high crystallinity of the synthesized TiO_2 photocatalysts. The XRD patterns of the Ru-doped TiO_2 system revealed peaks at $2\theta = 25.33^\circ, 37.75^\circ, 48.13^\circ, 56.62^\circ,$ and 62.68° . These peaks correspond to the (101), (004), (200), (211), and (002) planes of anatase TiO_2 , respectively (JCPDS card no. 21-1272). Interestingly, peaks associated with rutile phase and brookite phase ($2\theta = 30.80^\circ$) (JCPDS card no. 29-1360) were not present in all Ru-doped TiO_2 photocatalysts. This observation suggests that the presence of ruthenium ions affected the phase transformation from rutile to anatase phase. Moreover, there were no observable peaks of Ru metal (Ru^0) over TiO_2 or ruthenium oxide (RuO_2) which may be due to the low amount of ruthenium loading. The mass fraction of rutile (X_R) which was calculated from the XRD pattern are presented in Table I. The undoped TiO_2 sample gave the highest rutile content as compared to the Ru-doped TiO_2 photocatalyst. The crystallite grain sizes of the photocatalysts and effect of metal doping on TiO_2 phase transformation are shown in Table I. The crystal size determined from Scherrer formula for undoped TiO_2 was calculated to be 217.3 nm. Interestingly, doping of ruthenium ions at 0.002 mol ratio was observed to

dramatically decrease the crystal size to 28.96 nm Ru- TiO_2 . Further increasing the Ru: TiO_2 mol ratio from 0.005 to 0.008 gave almost comparable crystal size. These results suggest that doping ruthenium ions to TiO_2 via sol-gel synthesis enhances the formation of anatase TiO_2 and decreases the crystal size. These are desirable photocatalytic properties of the TiO_2 for photodecolorization processes.

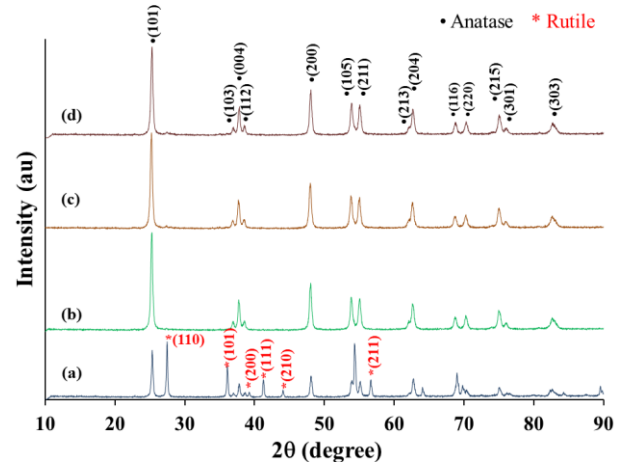


Fig. 3. X-ray diffraction pattern for (a) undoped TiO_2 showing rutile and anatase crystallographic planes, (b) 0.002 Ru- TiO_2 , (c) 0.005 Ru- TiO_2 , (d) 0.008 Ru- TiO_2 . The photocatalysts were calcined at 500°C .

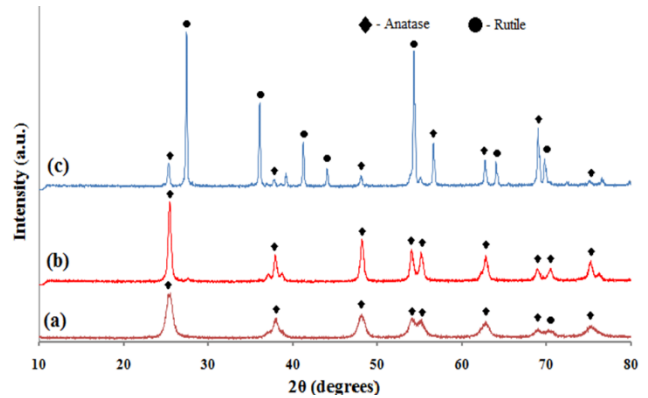


Fig. 4. X-ray diffraction patterns for 0.008 Ru- TiO_2 calcined at (a) 300°C , (b) 500°C , and (c) 700°C .

TABLE I: STRUCTURAL PROPERTIES OF UNDOPED TiO_2 AND Ru- TiO_2 . THE VALUES WERE DETERMINED ACCORDING TO ANALYSIS OF XRD

Samples	Rutile Mass Fraction (X_R)	Crystal Size (nm)
Undoped TiO_2	0.540	217.3
0.002 Ru- TiO_2	0.055	28.96
0.005 Ru- TiO_2	0.058	27.14
0.008 Ru- TiO_2	0.072	27.11

Fig. 4 shows diffractogram of 0.008 Ru- TiO_2 photocatalysts which were calcined at 300°C , 500°C , and 700°C . The XRD patterns for 0.008 Ru- TiO_2 calcined at 300°C and 500°C shows no observable peak at $2\theta = 27.34^\circ$ which indicates that no rutile phase formed in the photocatalysts. However, the peaks for 0.008 Ru- TiO_2 calcined at 500°C were narrower and more intense as shown in Fig. 4 (b) compared to 0.008 Ru- TiO_2 calcined at 300°C . These results suggest an incomplete crystallization of Ru- TiO_2 when calcined at 300°C [15]. The diffractogram for 0.008 Ru- TiO_2 calcined at 700°C showed an almost similar XRD pattern for undoped TiO_2 . The XRD pattern revealed peaks at $2\theta = 27.34^\circ, 36.01^\circ, 41.29^\circ, 44.05^\circ, 54.31^\circ, 63.91^\circ$

and 69.07° which corresponds to (110), (101), (111), (210), (211), (002), and (112) planes of the rutile phase [16],[17]. These results suggest that the formation of rutile phases is significantly affected by calcination temperature. Pure bulk anatase was previously shown to irreversibly transform to rutile in air at temperature $\sim 600^\circ\text{C}$ [18], [19].

2) Scanning electron microscopy and energy dispersive X-ray

The SEM images and EDS of Ru-TiO₂ are shown in Fig. 5 (a-c). The SEM images show that the titania particles are agglomerated and have different shapes and sizes. The high polydispersity of particles might be due to the grinding process after the calcination step.

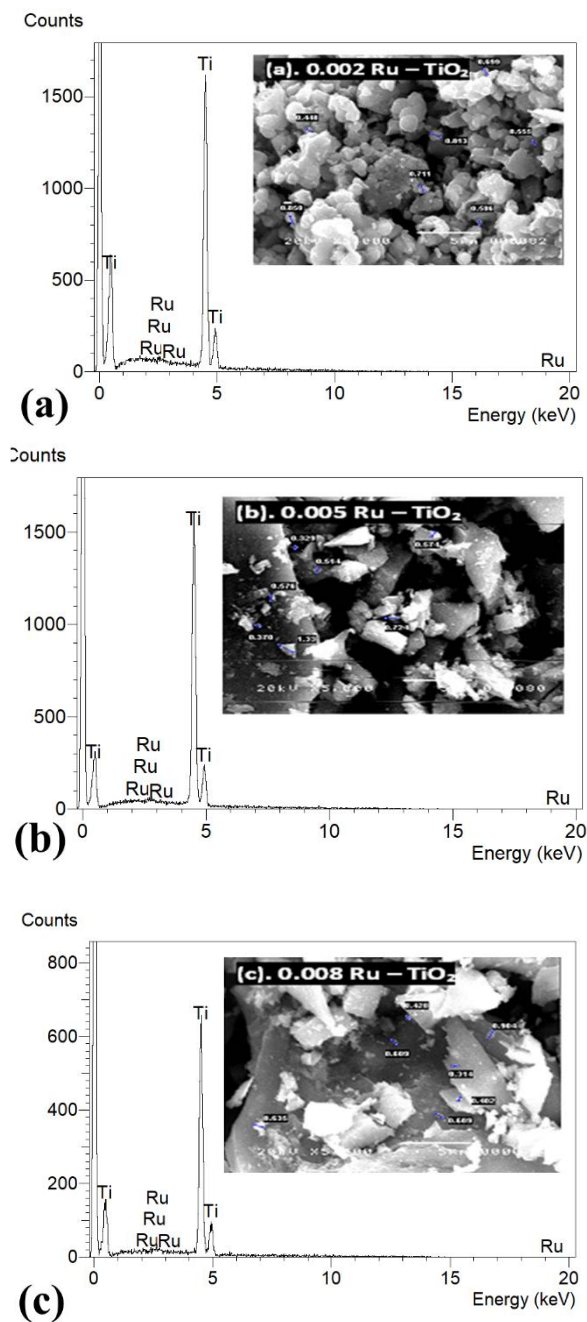


Fig. 5. EDS of (a) 0.002 Ru-TiO₂, (b) 0.005 Ru-TiO₂, (c) 0.008 Ru-TiO₂. The figure insets are their corresponding SEM images.

Fig. 5 (a) inset shows that the particle morphology for 0.002 Ru-TiO₂ is spherical as compared to the other Ru-TiO₂

photocatalysts. SEM images revealed irregularly shaped particle morphologies for 0.005 Ru-TiO₂ and 0.008 Ru-TiO₂. The observed irregular morphologies of the particles might be due to the uneven grinding of the photocatalyst using a simple mortar and pestle. Energy Dispersive X-ray Analysis was performed to confirm the presence of ruthenium ions on TiO₂ lattice. Peaks associated with titanium are evident from the spectra in the 4.0-5.0 keV region. The existence of ruthenium in the TiO₂ photocatalysts are confirmed by peaks in the 2.2-3.3 keV region. These results suggest the successful preparation of Ru-TiO₂ photocatalysts.

3) Fourier transform -infrared spectroscopy

The FT-IR spectra of undoped and ruthenium-doped photocatalysts are shown in Fig. 6 (a-d). The spectra of all photocatalysts showed no peaks in the region 4000 cm⁻¹ to 500 cm⁻¹ suggesting the absence of adsorbed water molecules and organic matter. However, a strong peak was observed in the region 450 cm⁻¹ to 500 cm⁻¹ which is due to the vibrational mode of Ti-O-Ti [20]. The FT-IR spectra of the undoped and ruthenium-doped photocatalysts agree with the previously reported infrared spectra for TiO₂ [12].

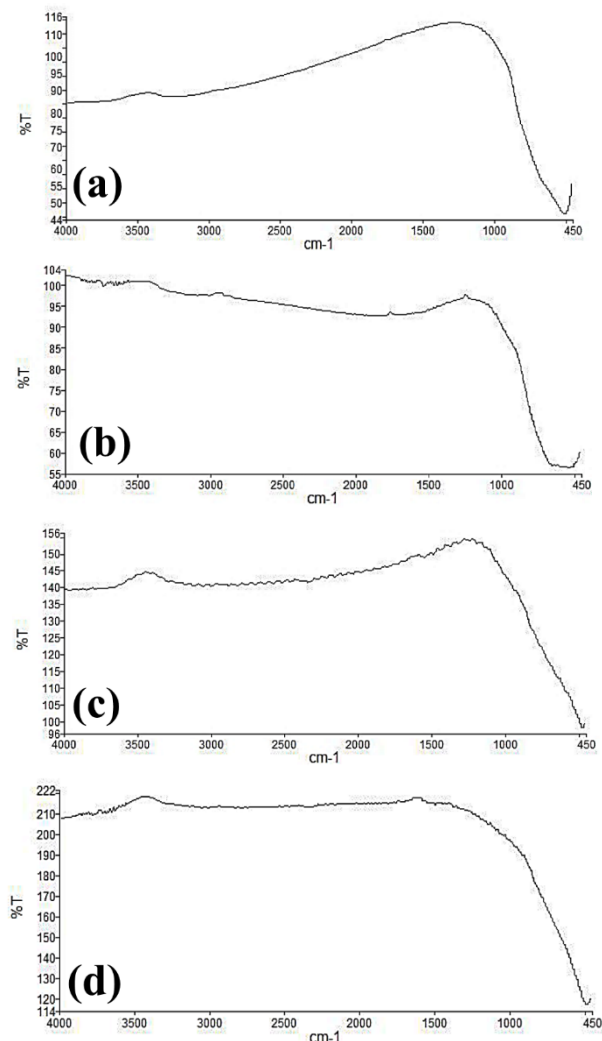


Fig. 6. FT-IR spectra of (a) undoped TiO₂, (b) 0.002 Ru-TiO₂, (c) 0.005 Ru-TiO₂, and (d) 0.008 Ru-TiO₂.

B. Photodecolorization of MG under Visible Light Illumination

1) Effect of dopant concentration

The absorbance of MG was monitored at $\lambda = 616$ nm during photocatalytic experiment and their corresponding concentration at time (t) were determined. All Ru-TiO₂ photocatalysts showed enhanced photodecolorization of MG compared to undoped TiO₂ (blue line) as shown in Fig. 7 (a-d). The undoped TiO₂ showed minimal decrease in MG concentration within 165 minutes of irradiation period. This is expected because undoped TiO₂ can only be activated with UV irradiation. The increment of the decrease in the concentration MG was observed to be greater when 0.008 Ru-TiO₂ was used as compared to 0.002 Ru-TiO₂ and 0.005 Ru-TiO₂. These results suggest significant enhancement in the visible light photocatalytic activity upon doping TiO₂ lattice with ruthenium metal.

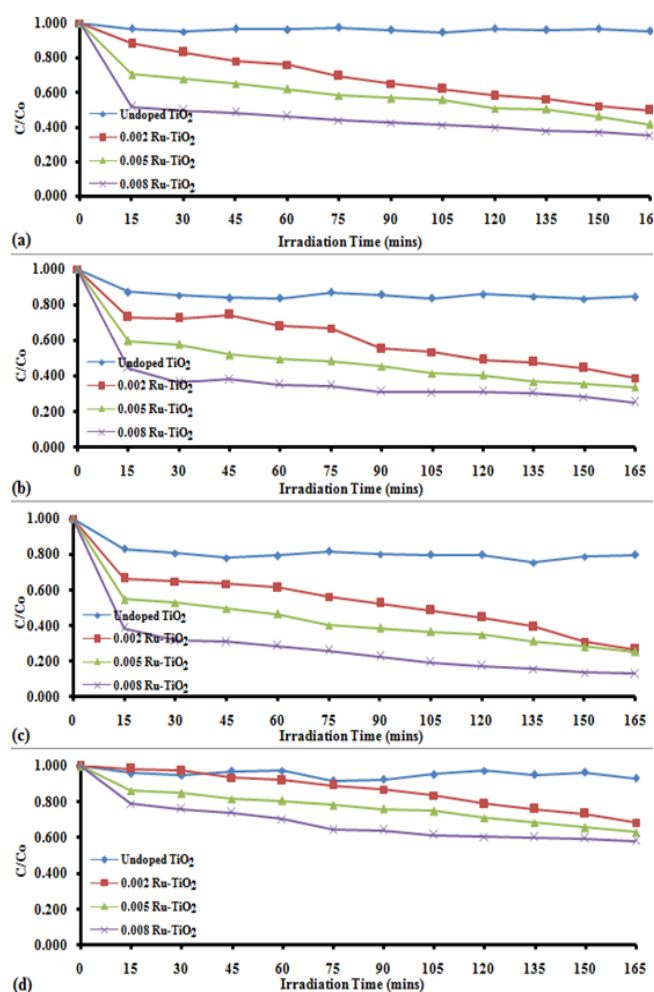


Fig. 7. Photocatalytic decolorization of 50 ppm MG solution using catalyst loading of (a) 0.50 g·L⁻¹, (b) 1.00 g·L⁻¹, (c) 1.50 g·L⁻¹, and (d) 3.00 g·L⁻¹.

The analysis of Figure 8 (a-d) also showed that increasing the amount of ruthenium dopant from 0.002 to 0.008 Ru:TiO₂ mol ratio led to higher photodecolorization efficiency. The addition of small amounts of transition metals such as Co, Cr, Cu, Fe, Mo, V, W, and Zn was previously shown to reduce the TiO₂ energy band gap, reduce the rate of electron-hole recombination process, and move the photon absorption to the visible region [16], [21]. These processes enhanced the photocatalytic oxidation efficiency of transition metal doped

TiO₂ with visible light illumination. Barakata and colleagues (2005) synthesized Co-doped TiO₂ and suggested that Co (III) ions functioned as electron scavengers that inhibited electron-hole (e⁻-h⁺) recombination, which ultimately led to a higher photocatalytic efficiency [22]. When the concentration of the dopant ions exceeds a certain optimal value, the photocatalytic activity decreases [11]. At high dopant metal concentrations, the transition metal becomes the center of charge recombination, which results reduction in photocatalytic efficiency. However, this decrease in photocatalytic efficiency due to high ruthenium doping concentration to TiO₂ was not observed in the present study.

2) Effect of photocatalyst loading

Fig. 8 shows the photodecolorization efficiency (*i.e.*, percent removal) of MG based on undoped TiO₂, varying Ru:TiO₂ mol ratio, and catalyst loading. The undoped TiO₂ exhibited lower percent removal of MG than Ru-TiO₂ catalysts. The percent MG removal of <20% was achieved using undoped TiO₂ is interesting at first sight because bare TiO₂ is not activated by visible light. However, this behavior can be attributed either to the adsorption of MG on the catalyst surface or the photosensitization of MG by visible light irradiation (see section C). On the other hand, all Ru-TiO₂ catalysts showed enhanced percent removal of MG as compared to undoped TiO₂.

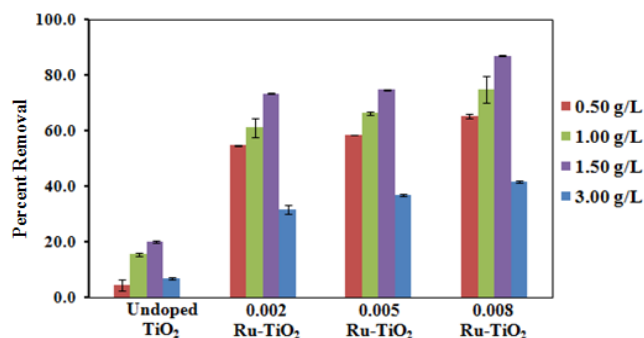


Fig. 8. Comparison of percent removal of 50 mg·L⁻¹ MG after 165 minutes of visible light illumination using different catalyst loading for undoped TiO₂, 0.002 Ru-TiO₂, 0.005 Ru-TiO₂, and 0.008 Ru-TiO₂.

Fig 8 also shows that increasing the photocatalyst loading from 0.5 g·L⁻¹ to 1.50 g·L⁻¹ also increased the percent removal of MG. The maximum percent removal of 86.98% was achieved with 1.50 g of TiO₂ per 1.0 L of MG solution and 0.008 Ru-TiO₂. The higher percent removal of MG with increasing catalyst loading is expected because of the greater number of active sites available for the generation of hydroxyl radicals and superoxide radicals for photocatalytic oxidation process [23]. However, a significant decrease in the percent removal of MG was observed when the catalyst loading was increased to 3.00 g·L⁻¹ loading. This reduction in the photodecolorization of MG beyond 1.50 g·L⁻¹ may be attributed to the excessive loading of catalyst which can weaken the penetration of visible light into the solution resulting in a hindered photocatalysis. Moreover, the increase in catalyst loading beyond optimum loading may result in the agglomeration of catalyst particles, which renders the catalyst surface unavailable for photon absorption leading to lower decolorization rate [24].

Interestingly, a study that used TiO₂ co-doped with C and

2.01 wt% Fe showed a degradation efficiency of ~78% under visible light irradiation as compared with the pure TiO₂ [25]. In a recent study, ternary Ag/ZnO/TiO₂ nanocomposite was synthesized *via* hydrothermal method. It was observed that the photocatalytic effect of the zinc doped TiO₂ nanocomposite exhibited 99.85% degradation on methylene blue, 98.41% on the malachite green after 120 min visible light irradiation, and 99.29% for rhodamine B after 60 min [26]. Our present results suggest that Ru-TiO₂ photocatalysts provided a simpler alternative compared to co-doped (Fe, C) TiO₂ and ternary TiO₂ nanocomposites for remediation of dye colored water.

3) Effect of calcination temperature of TiO₂ to its photocatalytic activity

The photodecolorization of 50 ppm MG using 0.008 Ru-TiO₂ photocatalysts calcined at 300°C, 500°C, and 700°C are shown in Fig. 9. The concentration of MG showed a decreasing concentration trend for all photocatalysts calcined at 300°C, 500°C, and 700°C. Interestingly, the Ru-TiO₂ calcined at 500°C showed the most significant decrease in MG concentration with time. This corresponds to a photodecolorization of ~87% after 165 minutes of visible light irradiation. The Ru-TiO₂ calcined at 700°C showed the lowest decrease in MG concentration. This behavior of the photocatalyst is attributed to the phase transformation of anatase to rutile phase of TiO₂ at 700°C as confirmed by XRD measurements. Hence, the formation of rutile phases adversely impacted the photodecolorization of MG. This data further supports the previous research which suggests that an increase in anatase content in TiO₂ leads to an increase in photocatalytic oxidation efficiency [27]. Furthermore, the catalytic activity of the N-doped TiO₂ was shown to decrease at a calcination temperature of 700°C. It was suggested that the mixtures of anatase and rutile have little photocatalytic activity compared to pure anatase TiO₂ [24]. The photodecolorization of MG using Ru-TiO₂ catalysts calcined at 300°C was lower compared to those calcined at 500°C. The photodecolorization efficiency of MG was calculated ~15% after 165 minutes of visible light irradiation. This observation can be attributed to the incomplete crystallization of the TiO₂ at 300°C.

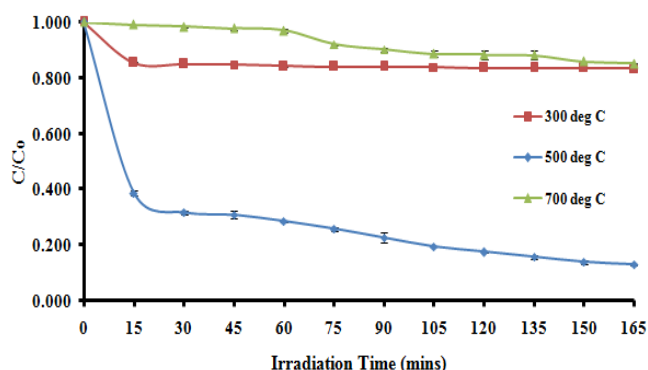


Fig. 9. Comparison of photodecolorization of 50 ppm MG solution using Ru-TiO₂ photocatalysts calcined at 300 °C, 500 °C, and 700 °C.

C. Visible Light Absorption and Proposed Mechanism of MG Photodecolorization

The photocatalytic decolorization of MG takes place based

on the proposed mechanism shown in Fig. 10 (a). Undoped titania cannot be activated by visible light because of the large band gap, hence, the observed photodecolorization can be initiated by MG absorption of visible light and electronic excitation. The structure of MG contains delocalized π bonds due to the aromatic functional groups. The extended π conjugation in MG would have a small energy gap between the highest occupied molecular energy level (HOMO) and lowest unoccupied molecular orbital (LUMO), thus making absorption of visible light possible. Moreover, the π orbitals in MG can interact with the $3d$ orbitals of Ti⁴⁺ [28],[29]. This electronic coupling leads to a complexation of MG on the TiO₂ surface. Therefore, it is plausible that the surface complex of MG and titania is excited by visible light, leading to an electron transferred from the LUMO of MG into the conduction band (CB) of TiO₂ with a lower energy level [30]. The electrons in the CB of TiO₂ reacts with O₂ to produce superoxide radical anion (O₂^{•-}) of oxygen that can react with MG molecules. Furthermore, the O₂^{•-} can be transformed into two more hydroxyl radicals (•OH). The resultant •OH species has the potential to degrade the MG dye and form stable species under visible light illumination [30]. However, this photodecolorization mechanism only accounted for <20% removal efficiency of MG with the experimental conditions in this study.

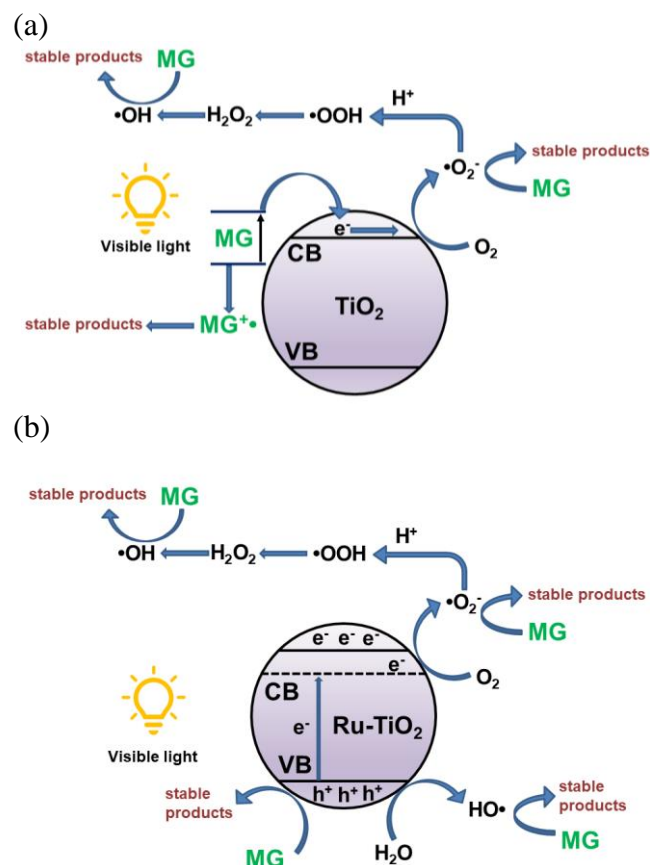


Fig. 10. Schematic diagram of proposed mechanistic pathway for photocatalytic decolorization of MG on (a) undoped TiO₂ and (b) Ru-TiO₂ with visible light illumination.

The photocatalytic activity of Ruthenium-doped TiO₂ is higher than undoped TiO₂ with visible light. The proposed mechanism for the decolorization of MG with visible light

illumination is shown in Fig. 10 (b). In general, doping of small amounts of transition metals to TiO₂ results in a lowering in the conduction band and reducing the energy band gap of TiO₂ [29], [31]. For transition metals such as Fe, Cr, and V, the level of the *d* electron energy is lower than the 3*d*-orbital energy of TiO₂ and located between the conduction and valence bands of TiO₂. Consequently, these transition metal doped TiO₂ are expected to be photoactivated by absorption of longer wavelengths of light compared to pristine TiO₂ [29]. The presence of Ruthenium in TiO₂ introduces additional acceptor levels in between the valence band (VB) and CB levels in TiO₂ [12], [32]. This additional level between the VB and CB causes the electrons to be promoted from the VB to the acceptor level, thus enhancing the separation of holes and electrons [23], [30]. When a Ru-TiO₂ is exposed to visible radiation, electrons are promoted from the valence band to the acceptor level which results in an electron-hole pair being produced as shown in Fig 10 (b). Ruthenium doping effectively captures photogenerated electrons and inhibits the electron-hole recombination, leading to enhanced photocatalytic activity. These entities can migrate to the catalyst surface, where they can participate in a redox reaction with other species present on the surface. In most cases, holes (h⁺) can react easily with surface bound H₂O to produce ·OH radicals. The e⁻ can react with O₂ to produce superoxide radical anion of oxygen (O₂^{·-}). The ·OH produced in these processes can then react with the MG to form stable species which leads to the decolorization of the MG solution. A recent study by Li and colleagues (2021) revealed that visible light excitation of ZnFe₂O₄/TiO₂ produced ·O₂⁻ free radicals that efficiently degraded the MG aromatic hydrocarbons and cleave benzene rings to small and biodegradable and colorless organic molecules. Moreover, the ZnFe₂O₄/TiO₂ can degrade up to 90.1% MG after 240 min visible light irradiation [33].

D. Kinetic Measurement

The analysis of kinetic parameters for the photocatalytic decolorization of MG by doped and Ru-TiO₂ photocatalysts was investigated and the obtained data were fitted by a pseudo first order kinetic equation:

$$\ln = \frac{C_o}{C} = kt \quad (4)$$

where C_o (mg·L⁻¹) is the initial MG concentration before irradiation, C (mg·L⁻¹) is the MG concentration at any time t (min) under visible light irradiation and k (min⁻¹) is the pseudo-first-order rate constant. The plots of $\ln(C_o/C)$ versus t for the different dopant concentrations and catalyst loadings are shown in Fig. 11 (a-d). The values of k_{app} were obtained by applying a least-squares regression analysis. In general, a plot of $\ln C/C_o$ versus time gives a linear relationship as indicated by the values of the correlation (R^2) obtained which are near to 1.0. This observation indicates that the decolorization of MG followed pseudo-first order kinetics.

The rate constant values were obtained for the Ru-TiO₂ photocatalysts and different catalyst loading are shown in Table II. Among the ruthenium-doped photocatalysts, a catalyst loading of 1.50 g·L⁻¹ gave the higher rate constants regardless of the Ru: TiO₂ mol ratio of the photocatalyst. The

highest rate constant of $7.29 \times 10^{-3} \text{ min}^{-1}$ was obtained at a catalyst loading of 1.50 g·L⁻¹ for 0.008 Ru: TiO₂. The differences in the rate constant values of various Ru-TiO₂ catalysts at different catalyst loading clearly shows the advantage of doping of ruthenium metals in TiO₂ lattice for photocatalysis under visible light. Furthermore, the dependence of the rate constant on catalyst loading also represents the importance of determining the optimal catalysts loading during photocatalytic experiments.

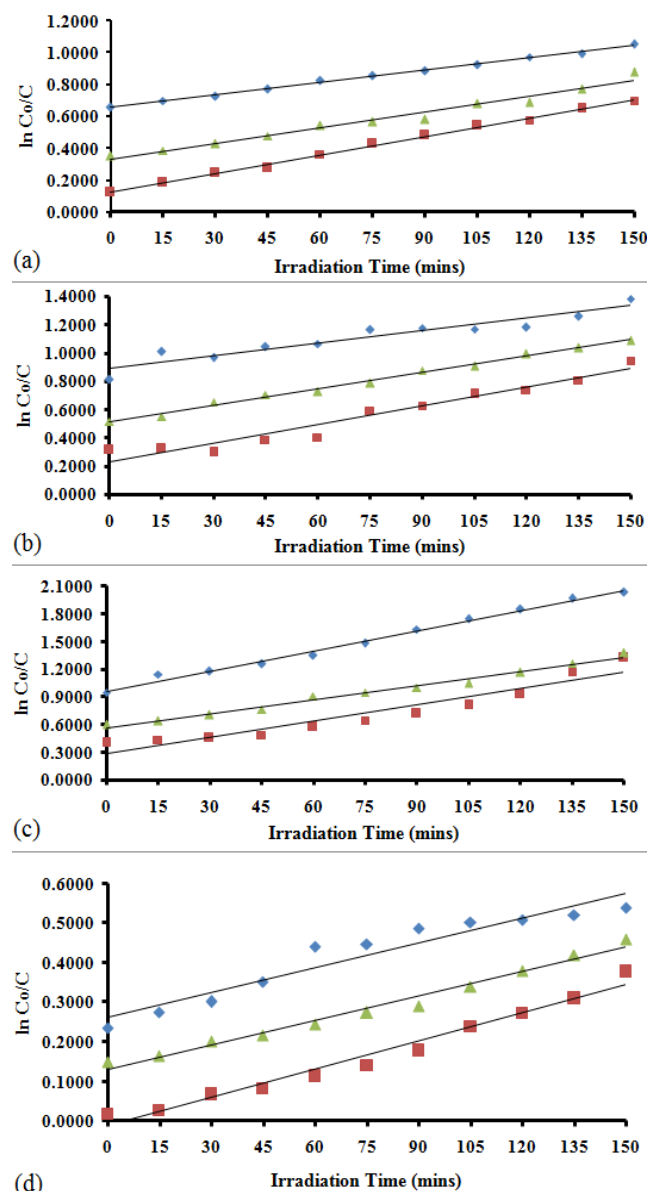


Fig. 11 Kinetics of malachite green with (a) 0.50 g/L, (b) 1.00 g/L, (c) 1.50 g/L, and (d) 3.00 g/L catalyst loading during photodecolorization. Legend: ■ - 0.002 Ru-TiO₂, ▲ - 0.005 Ru-TiO₂, ◆ - 0.008 Ru-TiO₂.

TABLE II: CALCULATED RATE CONSTANT VALUES IN THE PHOTOCATALYTIC DECOLORIZATION OF 50 PPM MG USING RU-TiO₂

Catalyst Loading (g·L ⁻¹)	Dopant Concentration	K_{app} (min ⁻¹)	R^2
0.50	0.002	3.86×10^{-3}	0.997
	0.005	3.27×10^{-3}	0.974
	0.008	2.59×10^{-3}	0.996
1.00	0.002	4.43×10^{-3}	0.947
	0.005	3.87×10^{-3}	0.992
	0.008	2.97×10^{-3}	0.904

1.50	0.002	5.90×10^{-3}	0.909
	0.005	5.12×10^{-3}	0.986
	0.008	7.29×10^{-3}	0.991
3.00	0.002	2.38×10^{-3}	0.975
	0.005	2.06×10^{-3}	0.982
	0.008	2.10×10^{-3}	0.923

IV. CONCLUSION

A significant enhancement in the photocatalytic activity of TiO₂ for the photodecolorization of MG was achieved using ruthenium-doped TiO₂ under visible light irradiation. The formation of undoped TiO₂ and the successful doping ruthenium ions into the TiO₂ lattice was confirmed by XRD, SEM-EDX and FT-IR studies. The doping of ruthenium ions to TiO₂ favored the formation of anatase TiO₂. The TiO₂ calcined at 500°C showed the highest photodecolorization of MG as compared to the photocatalysts calcined at 300°C and 700°C. Photocatalytic decolorization experiments revealed that increasing the catalyst loading from 0.5 g·L⁻¹ until 1.5 g·L⁻¹ led to a higher photodecolorization of MG. However, the photodecolorization efficiency decreased when the catalyst loading was 3.00 g·L⁻¹. The best parameters for the photodecolorization of MG was determined using 0.008 Ru:TiO₂ mol ratio, Ru-TiO₂ calcined at 500 °C, and catalyst loading of 1.5 g·L⁻¹. Under these conditions, a MG photodecolorization of 86.98% was achieved under visible light illumination. Kinetic studies also revealed that all the photocatalytic decolorization of MG followed pseudo-first order kinetics. Overall, our study presented a simple chemical synthesis method to develop a visible light responsive TiO₂ for the photodecolorization of MG. The Ru-TiO₂ photocatalysts has potential for application towards photocatalytic oxidation of other organic pollutants in water.

CONFLICT OF INTEREST

The authors declare no conflict of interest.

AUTHOR CONTRIBUTIONS

Sarah Jane C. Lopez and Ramon Victor M. Masangkay conducted the research; Aldrin Lorrenz A. Chan analyzed the literature data, wrote, and reviewed the paper; Lorico DS. Lapitan Jr. designed and supervised the research, analyzed the data, and edited the paper.

ACKNOWLEDGMENT

The authors would like to thank the following institutions where the material characterizations of the photocatalysts was conducted. SEM and EDS from Science Research Complex, De La Salle University, FT-IR from Department of Chemistry, Adamson University, XRD from Tokyo Institute of Technology, Department of Environmental Chemistry and Engineering, Suzukakadai Campus, Yokohama, Japan. The authors would like to thank Neal Adrian Cua, John Ryan Valen, and Gerard Hankiat Go for their support in material characterizations.

REFERENCES

- [1] H. Hosseini, H. Karimi, J. Foroughi, M. M. Sabzehmeidani, and M. Ghaedi, "Heterogeneous photoelectro-fenton using ZnO and TiO₂ thin film as photocatalyst for photocatalytic degradation malachite green," *Applied Surface Science Advances*, vol. 6, p. 100126, 2021.
- [2] R. V. Jadhav, D. Shrivastava, and K. Jadhav, "Microorganism-based treatment of azo dyes," *Journal of Environmental Science and Technology*, vol. 9, pp. 188-197, 2016.
- [3] F. de Andrade, A. B. de Oliveira, G. O. Siqueira, M. M. Lage, M. R. de Freitas, G. M. de Lima, and J. Nuncira, "MnFe₂O₄ nanoparticulate obtained by microwave-assisted combustion: An efficient magnetic catalyst for degradation of malachite green cationic dye in aqueous medium," *Journal of Environmental Chemical Engineering*, vol. 9, p. 106232, 2021.
- [4] S. Srivastava, R. Sinha, and D. Roy, "Toxicological effects of malachite green," *Aquatic Toxicology*, vol. 66, pp. 319-329, 2004.
- [5] V. Fessard, T. Godard, S. Huet, A. Mourrot, and J. M. Poul, "Mutagenicity of malachite green and leucomalachite green in in vitro tests," *Journal of Applied Toxicology*, vol. 19, pp. 421-430, 1999.
- [6] P. Geetha, M. S. Latha, and M. Koshy, "Biosorption of malachite green dye from aqueous solution by calcium alginate nanoparticles: Equilibrium study," *Journal of Molecular Liquids*, vol. 212, pp. 723-730, 2015.
- [7] E. Forgacs, T. Cserháti, and G. Oros, "Removal of synthetic dyes from wastewaters: A review," *Environment International*, vol. 30, pp. 953-971, 2004.
- [8] O. J. Hao, H. Kim, and P.-C. Chiang, "Decolorization of wastewater," *Critical Reviews in Environmental Science and Technology*, vol. 30, pp. 449-505, 2000.
- [9] A. Fujishima, T. N. Rao, and D. A. Tryk, "Titanium dioxide photocatalysis," *Journal of Photochemistry and Photobiology C: Photochemistry Reviews*, vol. 1, pp. 1-21, 2000.
- [10] C.-H. Chiou and R.-S. Juang, "Photocatalytic degradation of phenol in aqueous solutions by Pr-doped TiO₂ nanoparticles," vol. 149, pp. 1-7, 2007.
- [11] R. A. Elsalmony and S. A. Mahmoud, "Preparation of nanostructured ruthenium doped titania for the photocatalytic degradation of 2-chlorophenol under visible light," *Arabian Journal of Chemistry*, vol. 10, pp. 194-205, 2017.
- [12] J. A. I. Joice, T. Sivakumar, R. Ramakrishnan, G. Ramya, K. Prasad, and D. A. Selvan, "Visible active metal decorated titania catalysts for the photocatalytic degradation of Amidoblack-10B," *Chemical Engineering Journal*, vol. 210, pp. 385-397, 2012.
- [13] M. Senthilnathan, D. P. Ho, S. Vigneswaran, H. H. Ngo, and H. K. Shon, "Visible light responsive ruthenium-doped titanium dioxide for the removal of metsulfuron-methyl herbicide in aqueous phase," *Separation and Purification Technology*, vol. 75, pp. 415-419, 2010.
- [14] G. B. Song, J. K. Liang, F. S. Liu, T. J. Peng, and G. H. Rao, "Preparation and phase transformation of anatase-rutile crystals in metal doped TiO₂/muscovite nanocomposites," *Thin Solid Films*, vol. 491, pp. 110-116, 2005.
- [15] M. Ba-Abbad, A. A. Kadhum, A. B. Mohamad, M. Takriff, and K. Sopian, "Synthesis and catalytic activity of TiO₂ nanoparticles for photochemical oxidation of concentrated chlorophenols under direct solar radiation," *International Journal of Electrochemical Science*, vol. 7, pp. 4871-4888, 2012.
- [16] L. G. Devi, B. N. Murthy, and S. G. Kumar, "Photocatalytic activity of TiO₂ doped with Zn²⁺ and V⁵⁺ transition metal ions: Influence of crystallite size and dopant electronic configuration on photocatalytic activity," *Materials Science and Engineering: B*, vol. 166, pp. 1-6, 2010.
- [17] B. Yu, J. Zeng, L. Gong, M. Zhang, L. Zhang, and X. Chen, "Investigation of the photocatalytic degradation of organochlorine pesticides on nano-TiO₂ coated film," *Talanta*, vol. 72, pp. 308-314, 2007.
- [18] G. Li, L. Li, J. Boerio-Goates, and B. F. Woodfield, "High purity anatase TiO₂ nanocrystals: near room-temperature synthesis, grain growth kinetics, and surface hydration chemistry," *Journal of the American Chemical Society*, vol. 127, pp. 8659-8666, 2005.
- [19] T. B. Ghosh, S. Dhabal, and A. K. Datta, "On crystallite size dependence of phase stability of nanocrystalline TiO₂," *Journal of Applied Physics*, vol. 94, pp. 4577-4582, 2003.
- [20] W. Su, J. Zhang, Z. Feng, T. Chen, P. Ying, and C. Li, "Surface phases of TiO₂ nanoparticles studied by UV Raman spectroscopy and FT-IR spectroscopy," *The Journal of Physical Chemistry C*, vol. 112, pp. 7710-7716, 2008.
- [21] D. Paola, E. Garcia-López, S. Ikeda, G. Marci, B. Ohtani, and L. Palmisano, "Photocatalytic degradation of organic compounds in aqueous systems by transition metal doped polycrystalline TiO₂," *Catalysis Today*, vol. 75, pp. 87-93, 2002.
- [22] M. A. Barakat, H. Schaeffer, G. Hayes, and S. Ismat-Shah, "Photocatalytic degradation of 2-chlorophenol by Co-doped TiO₂

- nanoparticles,” *Applied Catalysis B: Environmental*, vol. 57, pp. 23-30, 2005.
- [23] G. Thennarasu, S. Kavithaa, and A. Sivasamy, “Photocatalytic degradation of orange G dye under solar light using nanocrystalline semiconductor metal oxide,” *Environmental Science and Pollution Research*, vol. 19, pp. 2755-2765, 2012.
- [24] U. Akpan and B. Hameed, “Parameters affecting the photocatalytic degradation of dyes using TiO₂-based photocatalysts: A review,” *Journal of Hazardous Materials*, vol. 170, pp. 520-529, 2009.
- [25] A. B. Lavand, M. N. Bhatu, and Y. S. Malghe, “Visible light photocatalytic degradation of malachite green using modified titania” *Journal of Materials Research and Technology*, vol. 8, pp. 299-308, 2019.
- [26] S. Kerli, M. Kavgacı, A. K. Soğuksu, and B. Avar, “Photocatalytic degradation of methylene blue, rhodamine-B, and malachite green by Ag@ ZnO/TiO₂,” *Brazilian Journal of Physics*, vol. 52, pp. 1-11, 2022.
- [27] A. S. Kovalenko, S. Y. Kuchmii, T. F. Makovskaya, A. V. Korzhak, V. V. Tsyryna, V. I. Yats'kiv, and V. G. Il'in, “Effect of Metal inclusions on the porous structure and photocatalytic activity of titanium dioxide,” *Theoretical and Experimental Chemistry*, vol. 39, pp. 119-125, 2003.
- [28] C. Chen, W. Ma, and J. Zhao, “Semiconductor-mediated photodegradation of pollutants under visible-light irradiation,” *Chemical Society Reviews*, vol. 39, pp. 4206-4219, 2010.
- [29] T. Umehayashi, T. Yamaki, H. Itoh, and K. Asai, “Analysis of electronic structures of 3d transition metal-doped TiO₂ based on band calculations,” *Journal of Physics and Chemistry of Solids*, vol. 63, pp. 1909-1920, 2002.
- [30] S. Wu, H. Hu, Y. Lin, J. Zhang, and Y. H. Hu, “Visible light photocatalytic degradation of tetracycline over TiO₂,” *Chemical Engineering Journal*, vol. 382, p. 122842, 2020.
- [31] Z. Yuan, J. Zhang, B. Li, and J. Li, “Effect of metal ion dopants on photochemical properties of anatase TiO₂ films synthesized by a modified sol-gel method,” *Thin Solid Films*, vol. 515, pp. 7091-7095, 2007.
- [32] W. C. Wu, C. S. Yang, and C. C. Chang, “Photo-degradation of salicylic acid over ruthenium oxide incorporated titania bifunctional photo-catalyst: An approach for direct cleavage of C_{aromatic}-O bond via hydro-deoxygenation,” *Molecular Catalysis*, vol. 478, p. 110560, 2019.
- [33] J. Li, Y. Huang, M. Su, Y. Xie, and D. Chen, “Dual light-driven p-ZnFe₂O₄/n-TiO₂ catalyst: Benzene-breaking reaction for malachite green,” *Environmental Research*, p. 112081, 2021.

Copyright © 2022 by the authors. This is an open access article distributed under the Creative Commons Attribution License which permits unrestricted use, distribution, and reproduction in any medium, provided the original work is properly cited ([CC BY 4.0](https://creativecommons.org/licenses/by/4.0/)).



Aldrin Lorrenz A. Chan was born in June 1993. Engr. Chan received his bachelor of science in chemical engineering from the Faculty of Engineering of the University of Santo Tomas, Manila, Philippines in 2014. Engr. Chan obtained his master of engineering science major in metallurgy in 2018 and master of science in

chemical engineering in 2019 through the dual-degree program of the University of Santo Tomas and Curtin University, School of Mines, Australia. Engr. Chan is currently affiliated with the Department of Chemical Engineering, University of Santo Tomas, Manila, Philippines, a licensed chemical engineer (registered by the Professional Regulations Commission) in the Philippines, and a member of the Philippine Institute of Chemical Engineers – Metro Manila Academic Chapter (PICHE-MMAC).



Sarah Jane C. Lopez was born in 1992. Engr. Lopez received his bachelor of science in chemical engineering from the Faculty of Engineering of the University of Santo Tomas, Manila, Philippines in 2013. Her undergraduate research project is on dye wastewater abatement using TiO₂ photocatalytic processes. Engr. Lopez is a licensed chemical engineer (registered by the Professional Regulations Commission) in the Philippines.



Arvie Victor Masangkay was born in 1992. Engr. Masangkay received his bachelor of science in chemical engineering from the Faculty of Engineering of the University of Santo Tomas, Manila, Philippines in 2013. His undergraduate research project centered on advanced oxidation processes for wastewater treatment using visible light responsive TiO₂. Engr. Masangkay is a licensed chemical engineer (registered by the Professional Regulations Commission) in the Philippines.



Lorico DS. Lapitan Jr. was born in October 1986. Lapitan studied at the University of Santo Tomas, Manila, Philippines from June 2003 to April 2007, where he earned his bachelor of science degree in chemistry. He then pursued his master of science in chemistry from the University of Santo Tomas with a scholarship from the Department of Science and Technology in the Philippines from June 2007 to April 2010. In 2018, Lapitan obtained his Ph.D. in chemistry from the University of Leeds, United Kingdom. Dr. Lapitan is currently an assistant professor at the Department of Chemical Engineering, Faculty of Engineering of the University of Santo Tomas, Manila, Philippines. Dr. Lapitan is a licensed chemist (registered by the Professional Regulations Commission) in the Philippines and an associate member of the National Research Council of the Philippines – Division X (Chemical Sciences). Dr. Lapitan has published several scientific articles and presented many international conference papers on nanomaterials and biosensor technology.